Smart Liposomal Drug Delivery for Treatment of Oxidative Stress Model in Human Embryonic Stem Cell-derived Retinal Pigment Epithelial Cells

Farnaz Behroozi, Mohammad-Jafar Abdkhodaie, Hamid Sadeghi Abandansari, Leila Satarian, Mohammad Kazemi Ashtiani, Mahmoud Reza Jaafari, Hossein Baharvand

PII: S0378-5173(18)30347-8
DOI: https://doi.org/10.1016/j.ijpharm.2018.05.056
Reference: IJP 17527

To appear in: *International Journal of Pharmaceutics*

Received Date: 14 January 2018
Revised Date: 18 April 2018
Accepted Date: 15 May 2018

Please cite this article as: F. Behroozi, M-J. Abdkhodaie, H.S. Abandansari, L. Satarian, M.K. Ashtiani, M.R. Jaafari, H. Baharvand, Smart Liposomal Drug Delivery for Treatment of Oxidative Stress Model in Human Embryonic Stem Cell-derived Retinal Pigment Epithelial Cells, *International Journal of Pharmaceutics* (2018), doi: https://doi.org/10.1016/j.ijpharm.2018.05.056

Smart Liposomal Drug Delivery for Treatment of Oxidative Stress Model in Human Embryonic Stem Cell-derived Retinal Pigment Epithelial Cells

Farnaz Behroozi[1], Mohammad-Jafar Abdkhodaie[1, *], Hamid Sadeghi Abandansari[2], Leila Satarian[3], Mohammad Kazemi Ashtiani[2], Mahmoud Reza Jaafari[4, 5,*], Hossein Baharvand[3, 6,*]

1. Department of Chemical and Petroleum Engineering, Sharif University of Technology, Tehran, Iran.
2. Department of Cell Engineering, Cell Science Research Center, Royan Institute for Stem Cell Biology and Technology, ACECR, Tehran, Iran.
3. Department of Stem Cells and Developmental Biology, Cell Science Research Center, Royan Institute for Stem Cell Biology and Technology, ACECR, Tehran, Iran.
4. Nanotechnology Research Center, Pharmaceutical Technology Institute, Mashhad University of Medical Sciences, Mashhad, Iran.
5. Department of Pharmaceutical Nanotechnology, School of Pharmacy, Mashhad University of Medical Sciences, Mashhad, Iran.
6. Department of Developmental Biology, University of Science and Culture, Tehran, Iran.

***Correspondence**

Baharvand@Royaninstitute.org

and

abdmj@sharif.edu

and

JafariMR@mums.ac.ir

Abstract

Oxidative stress has been implicated in the progression of age-related macular degeneration (AMD). Treatment with antioxidants seems to delay progression of AMD. In this study, we suggested an antioxidant delivery system based on redox-sensitive liposome composed of phospholipids and a diselenide centered alkyl chain. Dynamic light scattering assessment indicated that the liposomes had an average size of 140 nm with a polydispersity index below 0.2. The percentage of encapsulation efficiency of the liposomes was calculated by high-performance liquid chromatography. The carriers were loaded with N-acetyl cysteine as a model antioxidant drug. We demonstrated responsiveness of the nanocarrier and its efficiency in drug delivery in an oxidative stress model of human embryonic stem cell-derived retinal pigment epithelial (hESC-RPE) cells. The modeled cells treated with diselenide containing liposomes loaded with 10 mM NAC, showed a better therapeutic effect with a cell metabolic activity of 90%, which was significantly higher compared to insensitive liposomes or NAC treated groups ($P<0.05$). In addition, the expression of oxidative-sensitive gene markers in diselenide containing liposomes groups were improved. Our results demonstrated fabricated smart liposomes opens new opportunity for targeted treatment of retinal degeneration.

Keywords: Redox sensitive**,** Liposome, Diselenide, Drug delivery, Human embryonic stem cells, Retinal pigment epithelium cells, Age macular degeneration

1. Introduction

Age-related macular degeneration (AMD) accounts for 8.7% of blindness worldwide (Cai et al., 2000). Its prevalence increases exponentially after the age of 70 (Damico et al., 2012). Elderly people may suffer from loss of photoreceptors in the central retina, which is associated with retinal pigment epithelium (RPE) apoptosis due to harmful oxidative stress and diminished antioxidant defenses (Roth et al., 2004). There is currently no effective treatment for the most common form of this disease (dry AMD). In recent years, human embryonic stem cells (hESCs) providing a number of clinically attractive features, including the capacity for indefinite self-renewal and the potential to differentiate into RPE in vitro [for review see (Parvini M, 2014)]. These hESC-derived RPE (hESC-RPE) cells are similar to native RPE in expression of markers, transcriptome, and function (Parvini M, 2014). These hESC-RPE cells are a promising source for the treatment of AMD diseases (Schwartz SD, 2015; Mandai M, 2017) and modeling of AMD diseases for testing potential proposed drug and carriers (Kaczara P, 2010).

The invention of drug delivery systems has a tremendous impact on medicine, especially the field of retinal drug delivery (Thrimawithana Thilini, 2011). Nanoparticle drug delivery systems show potential for treatment of dry AMD in the posterior segment of the eye due to their capability to overcome ocular barriers, enhance permeation, improve drug water solubility, decrease frequent drug administration, protect administered drugs, and enable sustained, targeted drug release (Delplace et al., 2015; Lin et al., 2015). The nano-based drug delivery systems such as nanoemulsions, niosomes, dendrimers, nanoparticle loaded contact lenses (Hsu et al., 2014), and liposomes have gained tremendous attention due to their ability to enhance bioavailability of drug in different route of administration including systemic, topical, and injected drugs (Sahoo et al., 2008). Among these, liposomes appear to be suitable candidates' due to their ability to

encapsulate both hydrophobic and hydrophilic drugs, biocompatibility, enhancement of drug retention, and localization. According to Hathout et al., multilamellar liposomes that contained acetazolamide were more efficient than naked drug in lowering intraocular pressure (Hathout et al., 2007). As reported by Shen and Tu, the ocular bioavailability of liposomal ganciclovir in rabbits was 1.7-fold higher compared to naked drug (Shen and Tu, 2007). Products such as Visudyne® (Sharman et al., 1999) are used to treat choroidal neovascularization in wet AMD. Smart liposomes, which release medications upon exposure to triggers, are of interest. Their spatial and temporal specificity could provide better local control over the release at the appropriate time and place (Torchilin, 2014). In AMD, a redox sensitive liposome could provide targeted controlled delivery of the drug to the retina, enhance drug efficacy, and reduce drug off-target. This was achieved by incorporation of reduction-sensitive lipid like conjugate into liposome (Goldenbogen et al., 2011). Also, phospholipase-triggered drug release that form liposomal carriers (Arouri et al., 2015; Davidsen et al., 2003), reduction triggered delivery with disulfide conjugates of poly (ethylene glycol) and phospholipids (Zalipsky et al., 1999), and redox-triggered liposomes built from a quinone-lipid conjugate have been reported (Farokhzad and Langer, 2009). Inspired by the success of disulfide bonds, selenium (Se), an element listed in the same family as S in the periodic table of elements (chalcogens), has recently attracted great attention for their reduction responsiveness and their sensitivity to low concentrations of oxidative agents. Se-higher sensitivity is due to weaker bond energy of the C-Se (244 kJ/mol) and Se-Se bonds (172 kJ/mol) compared to the C-S (272 kJ/mol) and S-S (240 kJ/mol) bonds (Song and Du, 2014). Despite numerous advantages, no work has reported the design of redox-sensitive liposomes containing diselenide linkages.

In this study, we designed a novel redox liposome formulation based on incorporation of a

diselenide to treat oxidative stress model in hESC-derived RPE cells. These liposomes contained an alkyl chain in combination with Egg L-α-phosphatidylcholine (Egg PC), as the membrane destabilizing component and 1,2-dio-leoyl-sn-glycero-3-phosphoethanolamine (DOPE). The diselenide containing liposome can disrupt at redox conditions and release its payload (Fig. 1). Physicochemical and biological characteristics of liposome were investigated for particle size, zeta potential, and morphology. furthurmore, oxidative-induced degradation, drug loading capacity, drug release, in vitro cytotoxicity, and in vitro anti-oxidative effects of the carrier were studied.

2. Materials and Methods

2.1. Materials

Egg L-α-phosphatidylcholine (Egg, Chicken), 1,2-dio-leoyl-sn-glycero-3-phosphoethanolamine (DOPE), 1,2-dimyristoyl-sn-glycero-3-phosphocholine (DMPC), and polycarbonate membrane filter were purchased from Avanti Polar Lipids, Inc. (Alabaster, AL, USA) and used without further purification. Tris(2-carboxyethyl)phosphine (TCEP), N,N'-dicyclohexylcarbodiimide (DCC), EtOH, 10-bromodecanoic acid, 4-(Dimethylamino)pyridine (DMAP), magnesium sulfate ($MgSO_4$), L-cysteine, 5(6)-Carboxyfluorescein (dye content 90%), dimethyl sulfoxide (DMSO), anhydrous tetrahydrofuran (THF), sodium borohydride ($NaBH_4$), selenium (Se), Dimethylformamide (DMF), streptavidin, HEPES buffer, sonic hedgehog (SHH), N-acetyl cysteine (NAC), 2,7-dichlorodihydrofluorescein diacetate and anti-mouse IgG-peroxidase were obtained from Sigma-Aldrich (Taufkirchen, Germany). Triton X-100 was purchased from Carl Roth (Karlsruhe, Germany). Phosphate-buffered saline (PBS), trypsin/EDTA, L-glutamine (L-Gln), DMEM/F12, knock-out serum, noggin, penicillin, and streptomycin were purchased Gibco

BRL (Rockville, MD, USA). Mouse anti-RPE65 was obtained from Abcam (ab13826, Cambridge, MA, USA). Goat anti-mouse Alexa fluor 546 was purchased from Invitrogen (Carlsbad, CA, USA). L-glutathione reduced (GSH), phosphotungstic acid, hydrogen peroxide (H_2O_2) solution 30% (w/w), and methanol were purchased from Merck (Darmstadt, Germany). Dialysis membrane 12 kDa MWCO was purchased from Spectrum (Houston, TX, USA). Nylon membrane filter was obtained from Sartorius (Germany). 3-(4,5-dimethylthiazol-2-yl)-2,5-diphenyltetrazolium bromide (MTS) was purchased from Promega (Madison, WI, USA). RNeasy Mini kit with on-column DNase I digestion was purchased from Qiagen (Germany). High Capacity cDNA Reverse Transcription Kit was purchased from Takara Bio (Shiga, Japan). Parafilm was purchased from Pechiney Plastic Packaging (Menasha, WI, USA). Matrigel was purchased from Corning (New York, USA). Basic fibroblast growth factor (bFGF) was purchased from Thermo Fisher Scientific (Boston, MA, USA). All other chemicals and solvents were of analytical grade.

2.2. Preparation of smart liposomes

2.2.1. Synthesis of diselenide

We prepared diselenide according to a previously described method (Fig. 2A) (Rafique et al., 2015). Briefly, elemental Se (0.157 g, 1.99 mmol) and $NaBH_4$ (0.152 g, 3.98 mmol) were placed in a two-neck round-bottom flask and mixed under nitrogen gas flow. The 98% EtOH (0.7 mL) was added to this mixture until complete dissolution of Se and the formation of a white-gray solid. Dimethylformamide (DMF) (4 mL) was then added to the stirring solution until a red-brown color formed, followed by continuous addition of commercial 80% EtOH (0.45 mL) with vigorous stirring until the end of gas production. Then, Se powder (0.157 g, 1.99 mmol) was

added to the solution and stirred until the powder completely dissolved, and we observed a clear dark-red solution. We added 10-bromodecanoic acid (1 g, 3.98 mmol) to this solution, which changed its color from red to yellow. After 24 h, the reaction was stopped by the addition of water (12 mL). The reaction mixture was extracted with diethyl ether (3×10 mL), and the extracted organic phase was washed with water (3×20 mL) and brine (15 mL). The organic phase was dried over $MgSO_4$ and filtered. The solvent was completely evaporated, leaving a yellow powder as the product with the following specifications and ^{1}HNMR results (Fig. 2B I,II) – yield: 65%; ^{1}H NMR ($CDCl_3$, 400 MHz, δ): 1.22 (m, 20H, -CH_2), 1.50 (m, 4H, -***CH*****$_2$**CH_2Se-), 1.6 (m, 4H, -***CH*****$_2$**CH_2COOH), 2.2 (t, 4H, -***CH*****$_2$**Se-), 2.8 (t, 4H, -***CH*****$_2$**COOH).

2.2.2. Liposome preparation

Liposomes were prepared by the thin lipid film hydration method, followed by extrusion and dissolving the lipids (40 mM) in chloroform. Briefly, we prepared a dry lipid film, by rotary evaporation of the chloroform solution, from Egg PC, diselenide (SeSe), and DOPE with the following molar ratios: DOPE:SeSe:Egg PC (60:10:30) (Lip1), DOPE:SeSe:Egg PC (60:20:20) (Lip2), DMPC:SeSe (80:20), and DMPC:SeSe (90:10). Afterwards, these combinations were freeze-dried (FreeZone Freeze Dry System, Labconco) for at least 4 h to remove any traces of the solvents. This dry lipid film was hydrated in PBS (pH 7.4) and a 4 mg/mL lipid concentration. The hydrated mixture was vigorously vortexed for 30 min to generate multilamellar vesicles from the dry film. These vesicles were extruded 11 times through a 200-nm pore size polycarbonate membrane filter, then through a 100-nm pore size polycarbonate membrane filter (Avanti Polar Lipids Inc., USA) to generate a uniform particle size. We

prepared two control groups, DOPE:Egg PC (60:40) and DMPC, by the above mentioned protocol.

2.3. Preparation of N-acetyl cysteine (NAC) loaded liposome

Liposome groups loaded with NAC were prepared as described earlier. The lipid film was hydrated with 2 mL of a 30 mg/mL NAC stock solution. The suspension was briefly sonicated, then extruded 11 times through 200 and 100 nm pore size polycarbonate membrane filters. Unloaded drug was separated from the liposomes by overnight dialysis against PBS (pH 7.4) using a cellulose ester membrane (MWCO: 12 kDa). The final formulation was sterilized by passage through a 0.45 µm syringe filter.

2.4. Preparation of carboxyfluorescein (CF) loaded liposome

First, we sought to determine the optimal formulation for the smart liposomes. We loaded different formulations with a hydrophilic dye and studied their release behavior upon exposure to H_2O_2. First, the dried lipid film was hydrated in PBS (pH 7.4) that contained 40 mM carboxyfluorescein (CF) to form multilamellar liposomes. Subsequently, the liposomes were extruded 11 times through a 200 nm, followed by a 100-nm pore size polycarbonate membrane filter to obtain liposomes of a uniform particle size. The liposomes were sterilized by passage through a 0.45 µm syringe filter.

2.5. Liposome size and zeta potential (ς)

The liposome size and size distribution were measured by dynamic light scattering (DLS) using a Zeta Plus Instrument (Brookhaven Instrument Corporation, Holtsville, NY, USA). The zeta

potential of the formulations was measured by a zeta Phase Analysis Light Scattering (PALS) system with an ultrasensitive zeta potential analyzer (Brookhaven Instruments, Holtsville, NY, USA). The liposome suspension was diluted as needed with PBS to measure the size and with 10 mM of NaCl (pH 7.4) to determine the zeta potential. All size and zeta potential measurements were performed in triplicate (Table 1).

2.6. Transmission electron microscopy (TEM)

We used negative staining of the liposomes to verify their size and morphology. The stained samples were examined by a JEM-2000CX (JEOL Ltd., Japan) transmission electron microscope that had an accelerating voltage of 15 kV. For the negative staining, we used a 400-mesh grid (EM fine-grid F400, Nisshin EM Co., Tokyo, Japan) with a carbon support film (10-20 nm in thickness), The grid was given a hydrophilic treatment. Samples were stained at room temperature (RT). A drop of liposomal solution, distilled water, and 1% phosphotungstic acid (Merck, Tokyo, Japan) was placed on Parafilm® (Pechiney Plastic Packaging Co., Menasha, WI, USA). The grid was placed into the liposomal drop (30 seconds), then in a distilled water drop for washing (10 seconds), and finally in a phosphotungstic acid drop for staining (10 seconds). Any excess solution was removed with filter paper (Kodama et al., 2010) (Anthony C., 2005).

2.7. N-acetyl cysteine (NAC) assay

We used HPLC to measure the NAC concentration against a standard curve according to previously reported procedure (Anthony C., 2005). A stock standard solution (1 mg/mL) was prepared by dissolving 25.0 mg of NAC in 25.0 mL of the mobile phase by ultrasound for 30 min. From this solution, we prepared a 30 mg/mL working standard by adding 300 µL of the

stock standard solution to 10.0 mL of the mobile phase. In addition, the stock standard solution was diluted with the mobile phase to give five standard solutions that contained varying concentrations of NAC (10.0, 20.0, 30.0, 40.0, and 50.0 µg/mL) to be used in the linearity study. All solutions were injected (n=3) into the HPLC system.

The HPLC method was performed on a Shimadzu LC system (Kyoto, Japan) equipped with a 214-nm detector and a 3.9 mm x 30 cm column that contained packing L1. The mobile phase was composed of 0.05 M KH_2PO_4 and acetonitrile (95:5 v/v and pH adjusted to 3.0 with phosphoric acid) pumped at a flow-rate of 1.0 mL/min, isocratic elution. The mobile phase was filtered through a 0.45 µm nylon membrane filter (Sartorius, Germany) and degassed before use. A 100 µL volume was injected and NAC was detected at 214 nm. All analyses were performed at RT (25±1ºC).

We dissolved the liposomes in methanol in order to measure the loaded NAC. We quenched the liposomes by using 50 µL liposome dissolved in 950 µL methanol and heated the solution at 67 ℃ for 10 min. Loading of NAC in the liposomal formulation was determined before and after purification by dialysis, and we calculated the percent of encapsulated NAC.

2.8. Carboxyfluorescein (CF) assay

Fluorescence measurements for CF were performed by an SLM-4000 spectrofluorometer (SLM Instruments, Urbana, IL, USA). The excitation wavelength of CF at 488 nm (1 nm slit-width) and emission wavelength at 530 nm were detected using a Corning 3-68 cutoff filter (Corning, NY, USA). The fluorescence standard was 20 nM of CF. Lysis of the liposomes was performed by addition of Triton X-100 detergent (final concentration: 0.5%).

2.9. N-acetyl cysteine (NAC) triggered release

In vitro release profiles of NAC from liposomes were investigated in two different buffers, PBS (0.01 mol/L, pH 7.4) and 0.1 wt.% H_2O_2, by using a dialysis bag diffusion technique. Lip1 (DOPE:SeSe:Egg PC (60:10:30))+NAC, Lip2 (DOPE:SeSe:Egg PC (60:20:20))+NAC, and Egg PC/DOPE were introduced into dialysis membrane tubing (MWCO: 12-14 kDa) and incubated in 25 mL of buffer at 37°C with stirring. At predetermined intervals, the samples were drawn from each buffer outside the dialysis bag and replaced by an equal volume of the same medium. The concentration of NAC in the solution was measured by HPLC.

2.10. Carboxyfluorescein (CF) triggered release

Ten µl of different CF loaded liposome formulations, DMPC and Egg PC/DOPE were incubated at 37°C with 100 µl of the freshly prepared H_2O_2 buffers for 10 min. Total concentrations of H_2O_2 ranged from 0 to 800 µM. Aliquots (10 µl) were subsequently diluted in 1 ml HEPES buffer (200 mM, pH 7.4) and the fluorescence was measured before and after addition of Triton X-100.

2.11. Cell culture

Passage-30 human embryonic stem cells (hESCs, Royan H6) were cultured as described (Baharvand et al., 2006). The hESCs were induced to neuroectoderm (NE) in induction medium that contained DMEM/F12 medium, 5% KOSR, 0.1% B-27 supplement, 2% N-2 (Invitrogen; which included recombinant insulin, human transferrin, sodium selenite, putrescine, and progesterone), 1% NEAAs, 2 mM L-Gln, 0.1 mM β-ME, and 10 ng/mL bFGF, supplemented with noggin (250 ng/mL, R&D) for 6 days (Zahabi et al., 2012). The cells were subsequently

grown without noggin for another 6 days in the same medium in the presence of bFGF (10 ng/ml) and decreasing concentrations of all-trans retinoic acid (RA, Sigma-Aldrich; 0.6 to 0.2 µM) to promote additional rosette formation. The medium was renewed every other day at these stages. Then, cells were exposed to 25 ng/mL bFGF along with 25 ng/ mL SHH (Sigma Aldrich, UK) in the absence of RA for an additional 6 days to give rise to what appeared to be neural tube (NT) like structure-organized rosettes that included lumen. On day 18, the culture was maintained in DMEM-F12 medium supplemented with 5% KOSR, 1% NEAAs, and 2 mM L-Gln. Half of the medium was renewed every 3 days. We observed pigmented areas from day 25 that increased with further culturing at passage 0. RPE were expanded as passage 1 by 10 min exposure to trypsin/EDTA. Purified RPE were seeded onto Matrigel-coated tissue culture plates and expanded for 10-15 days until the desired density, at which point the appropriate phenotype was achieved. For the phagocytosis assay, the RPE cells were incubated with 1 µm green fluorescent latex beads (1.0×10^9 beads/ml; Polysciences, Inc., Warrington, PA, USA) for 24 h at 37°C, after which they were washed three times with PBS/Tween and viewed with an inverted fluorescent microscope (X71 Olympus, Tokyo, Japan).

Immunofluorescence staining

We sought to characterize the hESC-RPE cells. Passage-1 hESC-RPE cells were fixed with 2% paraformaldehyde in PBS for 10 min, permeabilized for 10 min in 0.1% NP-40 substitute (Sigma-Aldrich) in PBS and blocked with 10% normal goat serum in PBS for 1 h, followed by an overnight incubation with RPE65 antibody (ab13826, Abcam, Cambridge, MA, USA) at 4°C. Cells were then washed 3 times for 15 min each time in 0.1% Tween/PBS, incubated with anti-mouse Alexa-594 for 1 h at RT, washed 3 times for 15 min each in 0.1% Tween/PBS and

mounted using VectaShield with DAPI (Vector Laboratories, Burlingame, CA, USA). Stained cells were examined under an inverted fluorescence microscope (X71 Olympus, Tokyo, Japan).

2.12. Oxidative stress modeling

We conducted the oxidative stress experiments as follows. hESC-RPE cell cultures that had been passaged for 15 days were plated in RPE medium. After the cells reached 80% confluency, they were treated with chemical oxidants for 24 h and 48 h. A stock solution of freshly prepared 0.1 wt. % H_2O_2 in deionized water was added to the medium to produce a range of final concentrations (0 μM to 750 μM). The cells were exposed to these stock solutions for 24 h and 48 h in order to measure cell metabolic activity (Hanus et al., 2013).

2.13. Cytotoxicity assay

2.13.1. Cytotoxicity assay for H_2O_2 treated hESC-RPE cells

The MTS assay was performed according to the manufacturer's protocol. For H_2O_2 cytotoxicity studies, hESC-RPE cell medium was replaced by either fresh medium or medium that contained various concentrations of H_2O_2. The cells were incubated for 24 h and/or 48 h. After the specified incubation period, the cells were washed three times with PBS. Then, MTS stock solution (20 μL/well MTS and 100 μL/well cell media) was added to the cells. After an additional 2 h incubation, we used a microplate reader (SpectraMax, M5, Sunnyvale, CA, USA) to measure absorbance of the formazan at 490 nm. Measurements were obtained from three replicated wells of the 96-well plate and used to calculate metabolic activity of the chemically-treated cells.

2.13.2. Cytotoxicity assay for liposomes

We conducted NAC and liposome cytotoxicity studies on the hESC-RPE cells. First, the cells were incubated with NAC, Egg PC/DOPE+NAC (5 mmol/L), Lip1+NAC (5 mmol/L), Lip2+NAC (5 mmol/L), Lip1 (5 mmol/L), and Lip2 (5 mmol/L) for 24 h. After removal of the media, the cells were washed and we performed the MTS assay as previously described.

2.13.3. Quantitative real-time PCR (qRT-PCR)

Total RNA was isolated from 3 replicates of the hESC-RPE treated cells by using TRIzol reagent (Takara) and chloroform according to the manufacturer's instructions. cDNA was produced by reverse transcription with a Takara kit. Quantitative real-time PCR (qRT-PCR) was performed on a 7900HT Sequence Detection System (Applied BioSystems, CA, USA) with a Fast SYBR Green Master Mix (Applied Biosystems, CA, USA). The gene expression levels was normalized to the reference gene *GAPDH* and analyzed by Prism software (Prism 6.01, GraphPad Prism) using the comparative Ct method, $2^{-\Delta\Delta Ct}$. Supplementary Table 1 lists the primer sequences (Applied Biosystems) for superoxide dismutase 1 (SOD1), superoxide dismutase 2 (SOD2), and catalase (CAT).

Intracellular ROS measurement assay was performed. hESC-RPE cells (1×10^4 cells/well) in 96-well plates were incubated with 0 µM and 200 µM H_2O_2 for 2h at 37 °C. They were then treated with 0 mM NAC ,10 mM NAC, Lip1/NAC and Lip 2/NAC. They were washed with PBS and incubated for 20 min at 37 °C in PBS containing 20 µM 2,7-dichlorodihydrofluorescein diacetate (Sigma Aldrich). Intracellular ROS production was measured on a fluorescence plate reader with an excitation of 485 nm and emission of 528 nm. The experiments were performed in triplicate and repeated three times.

2.14. Statistical analysis

Data were analyzed by GraphPad Prism version 6.01 (GraphPad Software, San Diego, CA, USA). Average results are shown as mean±standard deviation (SD). Descriptive statistics, the independent t-test, and post hoc test for one-way ANOVA were used for statistical analyses. Alternative nonparametric tests of the above statistical tests were conducted. Statistical significance was set at $P<0.05$.

3. Results and Discussion

3.1. Characterization of nanocarriers

In the first step, we synthesized diselenide by a reaction between 10-bromodecanoic acid and Se powder in the presence of $NaBH_4$. ^{1}H-NMR confirmed the formation of bis(decanoic acid)-diselenide by a shift in the peak at 3.40 ppm (–***CH$_2$***-Br of 10-bromodecanoic acid) to 2.86 ppm (–***CH$_2$***-Se- of bis(decanoic acid)-diselenide) as seen in Figure 2B (I,II). FTIR spectrum analysis further confirmed the synthesis by the presence of one band at 1734 cm^{-1}, which was related to -COO- band stretching vibrations in PCL and a broad band at 2500-3400 cm^{-1} that was assigned to the terminal carboxyl groups of the diselenide segments (Fig. 2C).

We studied liposome release behavior in different concentrations of H_2O_2 to find the optimal formulation. The two candidates were liposomes composed of DMPC and Egg PC/DOPE. Carboxyl fluorescent release was assessed by fluorescence measurements with an SLM-4000 spectrofluorometer (SLM Instruments, Urbana, IL, USA) at an excitation wavelength of 488 nm (1 nm slit-width) and an emission above 530 nm. The liposomes were exposed to varying

concentrations of H_2O_2 (0 to 800 µM) as well as Triton-X100. DMPC that lacked Se-Se bond showed negligible release, which agreed with our expectations (Fig. 3A). DMPC formulations that contained 10% and 20% diselenide did not show a significan difference in release when exposed to the various concentrations of H_2O_2 (Fig. 3A). However, DMPC formulations that contained 10% diselenide had no release at low concentrations of H_2O_2, which might be attributed to the low permeability of the liposome structure. DMPC that contained 20% diselenide released CF at a high concentration (800 µM H_2O_2). This observation indicated that DMPC responded only at the high concentrations of H_2O_2. For our delivery purposes, a carrier should release its load at low and high H_2O_2 concentrations covering both ends of the spectrum. Based on the above results, DMPC based liposomes seem to be effective only at high concentrations of H_2O_2, while, DOPE/Egg PC carriers show response at both low and high concentrations of H_2O_2.

We observed no release with the Egg PC/DOPE formulations (Fig. 3A). However, the DOPE/Egg PC that contained 10% diselenide had CF release was proportional to the concentration of H_2O_2. (Fig. 3A). By increasing H_2O_2 concentration, the amount of CF release increased as well. Interestingly, when we increased the diselenide concentration of the formula to 20%, we observed a sharper response of CF from our carrier after exposure to different concentrations of H_2O_2 (Fig. 3A). The data implied that the Egg PC/DOPE seemed to be a better candidate than DMPC since it was sensitive at low H_2O_2 concentrations compared to DMPC. In addition, this carrier had a linear release response that was a function of the H_2O_2 concentration. When we increased the diselenide concentration in the liposome bilayer for the Egg PC/DOPE, we observed a sharper release. Therefore, we chose this formulation for the rest of the study.

The physical characteristics of the carriers were evaluated. The unloaded liposomes had a mean diameter of less than 150 nm with a polydispersity index (PDI) below 0.2. All drug-loaded liposomes had mean diameters less than 170 nm and good polydispersity (PDI<0.2). The liposomes that did not contain diselenide had slightly negative zeta potentials; however, those with diselenide had significantly more negative charges (Table 1). The TEM results showed liposome with round morphology and size ranges of 100-140 nm, which is in accordance with the size acquired by DLS (Figure 3 B (I, II)). The encapsulation efficiency (EE) of NAC loaded liposomes was approximately 12%.

In this study, we prepared three different liposomal formulations, DOPE:SeSe:Egg PC (molar ratio: 60:10:30) (Lip1); DOPE:SeSe:Egg PC (molar ratio: 60:20:20) (Lip2); and DOPE:Egg PC (molar ratio: 60:40), that contained NAC with a lipid concentration of 40 mM. We observed no significant differences in formulation sizes and EE (Table 1). A stability study conducted over 28 days showed that the liposomes ranged between 155 ± 3.30 nm and 223.3 ± 2.89 nm, with a PDI of approximately less than 0.2. The DLS measurements of size and PDI of all groups showed that the liposomes had suitable size and homogeneity. The surface charges were approximately -3.51 ± 0.50 mV for liposomes that lacked diselenide and approximately -20 mV for those with diselenide. The negative surface charge was due to the presence of negatively charged phospholipids, which would be ideal for intravitreal injections of drugs to the posterior segment of the eye. The vitreous humor of the mammalian eye mainly consists of collagen, fibrils, glycosaminoglycans (GAGs), hyaluronic acid (HA), and heparin sulfate (HS). Both HA and HS carry negative charges. A charge dependent suppression on particle diffusion for positively charged nano-carriers has been reported (Käsdorf et al., 2015). Therefore, the negatively charged

liposome would be a suitable carrier for drug delivery to the posterior segment of the eye, particularly the retina, due to repulsive induced electrostatic forces (Käsdorf et al., 2015).

We examined the sensitivity of these liposomes by measuring the drug release at different redox environments. Their trigger drug release in two different buffers: PBS (0.01 mol/L, pH 7.4) and 0.1 wt. % H_2O_2 were measured by dialysis bag diffusion technique. The release profiles of drug-loaded liposomes that contained diselenide showed instant release of drug when exposed to 0.1 wt. % H_2O_2. Liposomes that lacked diselenide showed no release in these buffers. According to the above results, the liposomes with diselenide showed a reduction in triggered release of their load upon exposure to 0.1 wt. % H_2O_2, which was due to cleavage of the diselenide bond upon exposure to the reducing agents. This would disturb the vesicle membrane and allow release due to the formation of transient defects or structural rearrangements. The release of the loaded drug from the liposome was negligible without the reducing agent (Fig. 4).

Our data showed that the reduction kinetics is a function of the amount of diselenide bond present in the bilayer of the liposomes. Data from the first 15 min for liposomes with 20% diselenide (Lip2) showed that more than 50% of the load released upon addition of 0.1 wt. % H_2O_2. However, we observed 40% release of the drug from the liposomes that contained 10% diselenide (Lip1). This finding indicated that the rate of release in liposomes with 20% diselenide was slightly higher compared to 10% diselenide. This implied that the higher the concentration of sensitive linkage, the quicker the system would respond to the reducing agent. Release of drug from Egg PC/DOPE that lacked diselenide was negligible in the presence and absence of the reducing agent.

3.2. *In vitro* studies

The hESCs were induced to RPE cells according to the protocol by Zahabi et al. Followed by 10-15 days' culture in passage 1, the monolayer of RPE cells were observed (Fig. 5A). After 10 days of passaging, the cells rearranged in a regular hexagonal mosaic, with sufficient confluency to proceed with the oxidative stress modeling experiments (Fig. 5B). We performed the phagocytosis which in known as a critical function of RPE cells. Fluorescent microscopy analysis of the hESC-RPE cells after 24 h incubation with florescent latex beads demonstrated that the cells had the potential for phagocytosis. (Fig. 5C). In addition, data from immunostaining with anti-RPE65 implied that passage-1 RPE cells expressed significant levels of the mature RPE cell marker (Fig. 5D-F).

3.2.1 Cytotoxicity assay of carriers

hESC-RPE cells at passage 1 were divided into 5 groups (control, NAC, Lip1+NAC, Lip2+NAC, Egg PC/DOPE) for all experiments. We assessed the cytotoxicity of the Egg PC/DOPE, Lip1, and Lip2 in the presence and absence of NAC. The MTS assay was used to determine the effects of the hESC-RPE cells at total NAC concentrations that ranged from 0 to 10000 µM on healthy cells. Figure 5G shows that the DOPE/Egg PC liposome had a 15% toxicity effect at concentrations that ranged from 3 to 10 M on hESC-RPE cells. This result was similar to carriers that contained diselenide with or without NAC, which had a toxicity effect of approximately 5%-10%. This negligible difference among the groups might be due to the presence of diselenide and its therapeutic effects (Peter C. Raich, 2015; Jacek Młochowski, 2015). This negligible cytotoxic effect of the carriers indicated that liposomes could be suitable candidates for drug delivery.

3.2.2 Cytotoxicity assay of oxidative stress modeled hESC-RPE cells

The hESC-RPE cells were modeled using varying concentrations of H_2O_2 (0 to 750 µM) in an attempt to find the appropriate oxidative stress model to study the therapeutic effect of these carriers. Therefore, we used the MTS assay to assess metabolic activity of cells exposed to H_2O_2 after 24 h and 48 h. Figure 5H shows that the control groups (not treated with H_2O_2) had more than 99% metabolic activity. However, with increasing H_2O_2 concentration, the cell metabolic activity dropped to approximately 80%. At the 200 µM concentration of H_2O_2, cell metabolic activity decreased to approximately 35% in the 24 h and 50% in the 48 h treated groups ($P<0.01$). Increased concentration and longer exposure time of H_2O_2 caused higher mortality. Pretreatment with 500 µM of H_2O_2 caused a 50% decline in survival rate at 24 h, whereas there was a 70 % drop during 48 h exposure to H_2O_2 ($P<0.01$). We observed almost 20% metabolic activity at the 750 µM concentration of H_2O_2 for both 24 h and 48 h exposure time. Therefore, the groups treated for 24 h with 200 and 500 µM H_2O_2 were suitable since they had less cell death compared to the other groups. These levels of oxidative stress model different stages of AMD, which also evaluates the sensitivity of our carrier at low levels of stress.

3.2.3 Therapeutic effect of smart liposomes on oxidative stress modeled hESC-RPE cells

Previous studies reported that 10 to 20 mM of NAC had therapeutic effects on reducing oxidative stress in RPE cells (Gerona et al., 2010; Tate et al., 1995). For the therapeutic assay, hESC-RPE cells pretreated overnight with 200 and 500 µM H_2O_2 were exposed to different groups of carriers and naked drug (Fig. 6). The group pretreated with 200 µM of H_2O_2 had a cell survival of 70%; the group pretreated with 500 µM had a cell survival of 50% (previously reported). We intended to study the therapeutic effect and responsiveness of liposomes under

both reduction-oxidation conditions. The cells pretreated with 200 µM H_2O_2 were treated with liposomes. We observed that both diselenide containing liposomes, Lip1/NAC and Lip2/NAC, with 10 mM NAC, showed a better therapeutic effect with a cell metabolic activity of approximately 90%. It was was significantly higher compared to control group or NAC treated groups ($P<0.05$). We noted that for the 500 µM H_2O_2, the liposomes that contained 10% diselenide had a cell metabolic activity of approximately 70% and the liposomes with 20% diselenide had a cell metabolic activity of approximately 80%. Cell metabolic activity in both groups were significantly higher compared to the control ($P<0.05$) and NAC treated groups ($P<0.01$).

The data from the cells pretreated with 200 µM H_2O_2 showed that for low levels of oxidative stress, the smart carriers had the potential to mitigate cell death due to oxidative responsiveness of the liposomes. At higher levels of ROS, we observed that liposome treatments significantly enhanced cell survival. This finding was particularly noted in groups that had the higher concentration of diselenide (20%). This data indicated that the concentration of diselenide present in the liposomes could be an important variable for more extreme levels of oxidative stress, even though we observed satisfactory results for both groups of liposomes. On the other hand, the protective effect of the liposomes in prevention of NAC damage when exposed to free radicals might explain why smart liposomes showed a better therapeutic effect compared to NAC alone.

3.2.4 Gene expression levels of oxidative-sensitive markers in treated hESC-RPE cells

Reactive oxygen species develop oxidative stress, which contributes to the pathogenesis of AMD. RPE cells are considered a primary target in AMD. Enzymes such as *SOD1*, *SOD2*, and

CAT have key roles in protecting cells against oxidative stress and regulating ROS. Expressions of these enzymes in hESC-RPE cells were detected by qRT-PCR.

We evaluated the therapeutic effectiveness and responsiveness of the smart liposomes at low levels of oxidative stress by conducting a gene study test on cells treated with 200 µM of H_2O_2 rather than other groups of oxidative stress. After 24 h, the cells were treated with Lip2+NAC, Lip1+NAC, and Egg/DOPE with an NAC concentration of 10 mM. We also included a non-treated group and a group of healthy cells without any oxidative stress to find the treatment effect of the smart delivery system in regulating generated ROS in RPE cells.

As shown in Figure 7, expression of *SOD1* gene in the untreated cells was 5-fold lower than the healthy cells, whereas the NAC treated cells was approximately 3.3-fold lower than the healthy cells ($P<0.01$). In addition, the *SOD2* gene in the untreated cells was approximately 2.5-fold lower; for the NAC treated, they were approximately 2.5 and 2-fold lower than the healthy cells (Fig. 7; $P<0.01$). However, cells treated with Lip2+NAC and Lip1+NAC showed the similar expression levels for *SOD1* and *SOD2* to healthy cells. This finding indicated that cells induced with oxidative stress maintained normal levels of *SOD1* and *SOD2* when treated with smart liposomes loaded with NAC. The reason that naked drug had no significant treatment effect was possibly due to its sensitivity and degradation in the oxidative stress regions; therefore, when NAC is protected in a carrier like liposome it has better therapeutic effect. *CAT* expression of modeled cells treated with Lip2+NAC and Lip1+NAC did not significantly differ from healthy cells (Fig 7), whereas cells under oxidative stress that were untreated had a 2.2-fold increase and those treated with 10 mM NAC showed a 2-fold increase compared to healthy cells ($P<0.01$). Data from gene expressions indicated that NAC loaded smart liposomes seemed to effectively deliver NAC to the modeled cells, whereas naked drug or liposomes that lacked diselenide

seemed to be unsuccessful. This agreed with our observation from the drug release data, which implied that smart liposomes released their cargo upon exposure at the target site unlike liposomes that lacked the sensitive bond. The liposomes protected NAC from degrading in the oxidative stress regions.

In addition, treatment of hESC-RPE cells with H_2O_2 led to an increase in intracellular ROS levels compared with untreated cells. The intensity of the mean oxidized DCF peak was increased by 2.5-fold compared with controls after 200 μM H_2O_2 treatment in hESC-RPE cells. However, treatment with Lip 1/NAC and Lip 2/NAC attenuated the ROS accumulation level to the same value as intact cells, while treatment with naked NAC was as satisfying (Fig. S1).

4. Conclusion

The redox responsive liposome containing diselenide linkage was developed as an anti-oxidant carrier on oxidative stress model of hESC-RPE cells (Fig. 1). Smart liposomes showed a triggerable release of their content when exposed to oxidative stress regions while they had no cytotoxicity on cells. The protective effect of NAC, as anti-oxidant, was greater in hESC-RPE cells treated with smart liposomal NAC formulation compared to conventional methods. The protecting effect of liposome for loaded drug and high level release of anti-oxidant in response to oxidative stress, resulted in reducing ROS level and enhancing therapeutic effect. Taken together, our data demonstrate hESC-RPE cells induced with oxidative stress treated with smart liposomes loaded with NAC leads to increased anti-oxidant gene expression, resulting in RPE cell death prevention. These results strongly suggest an essential role of oxidative responsive liposomes, for delivering antioxidants to the diseased cells in order to boost cellular defense system, in maintaining the redox homeostasis in RPE cells. The proposed carrier is promising for

localized drug delivery. Although it is noteworthy to mention that for in vivo studies there is the concern for multiple intravitreal injections which cause side effects such as retinal detachment. We are hoping that such smart carriers will reduce the number of required injections and the caused side effects to a degree. We will also try topical administration of the liposomes in animal studies to evaluate the ability of the carriers to reach the posterior segment. Also, studies have demonstrated that the toxicity of diselenide depends on the type of species (rat or mice) and route of administration (i.p or s.c) (Nogueira et al., 2002). On the other hand, these compounds have been considered for potential use as pharmaceutical antioxidants, anti-inflammatory and antinociceptive (Anderson et al., 1994; Schewe et al., 1995). There is a lack of toxicity studies of Se organic forms which needs to be done. The mentioned above could be examined in future studies. The proposed carrier is promising for localized drug delivery.

Acknowledgments

This work was supported by grants from Royan Institute, the Iran National Science Foundation (INSF), and Iran Science Elites Federation to H. B.

Competing financial interests

The authors declare no competing financial interests.

References

Anderson et al., 1994. The effect of various antioxidants and other modifying agents on oxygen-radical-generated DNA damage in human lymphocytes in the COMET assay, Mutation Research/Fundamental and Molecular Mechanisms of Mutagenesis 1, 261-271.

Anthony C.,2005. Acetylcystein Assay.Pharmacopeial Forum 31, 726. http://www.pharmacopeia.cn/v29240/usp29nf24s0_m750.html

Arouri A, Trojnar J, Schmidt S, Hansen A.H., Mollenhauer J, Mouritsen O.G., 2015. Development of a cell-based bioassay for phospholipase A^2-triggered liposomal drug release. PLoS One 10, 1–13.

Baharvand H., Ashtiani S.K., Taee A, Massumi M, Valojerdi M.R., Yazdi P.E., Moradi S.Z., Farrokhi A., 2006. Generation of new human embryonic stem cell lines with diploid and triploid karyotypes. Dev. Growth Differ. 48, 117–128.

Cai J., Nelson K.C., Wu M, P.S., Jones D.P., 2000. Oxidative Damage and Protection of the RPE . Prog Retin Eye Res. 19, 205-21.

Cano M., Wang L., Wan J., Barnett B.P., Ebrahimi K., Qian J., Handa J.T., 2014. Oxidative stress induces mitochondrial dysfunction and a protective unfolded protein response in RPE cells. Free Radic. Biol. Med. 69, 1–14.

C.W Nogueira, E. B. Quinhones, E. A. C. Jung, G. Zeni, J. B. T. Rocha, 2002. Anti-inflammatory and antinociceptive activity of diphenyl diselenide, Inflamation research 52, 56-63.

Damico F.M., Gasparin, F., Scolari, M.R., Pedral, L.S., Takahashi, B.S., 2012. New approaches and potential treatments for dry age-related macular degeneration. Arq. Bras. Oftalmol. 75, 71–76.

Davidsen, J., Jørgensen K., Andresen T.L., Mouritsen O.G., 2003. Secreted phospholipase A2 as a new enzymatic trigger mechanism for localised liposomal drug release and absorption in diseased tissue. Biochim. Biophys. Acta - Biomembr. 1609, 95–101.

Delplace V., Payne S., Shoichet M., 2015. Delivery strategies for treatment of age-related ocular diseases: From a biological understanding to biomaterial solutions. J. Control. Release 219, 652–668.

Farokhzad O.C., Langer R., 2009. Impact of Nanotechnology on Drug Delivery. ACS Nano 3, 16–20.

Gerona G., López D., Palmero M., Maneu V., 2010. Antioxidant *N* -Acetyl-Cysteine Protects Retinal Pigmented Epithelial Cells from Long-Term Hypoxia Changes in Gene Expression. J. Ocul. Pharmacol. Ther. 26, 309–314.

Goldenbogen B., Brodersen N., Gramatica A., Loew M., Liebscher J., Herrmann A., Egger H.,

Budde B., Arbuzova A., 2011. Reduction-sensitive liposomes from a multifunctional lipid conjugate and natural phospholipids: Reduction and release kinetics and cellular uptake. Langmuir 27, 10820–10829.

Hanus J., Zhang H., Wang Z., Liu Q., Zhou Q., Wang S., 2013. Induction of necrotic cell death by oxidative stress in retinal pigment epithelial cells. Cell Death Dis. 4, 1–11.

Hsu K.H., Gause S., Chauhan A., 2014. Review of ophthalmic drug delivery by contact lenses. J. Drug Deliv. Sci. Technol. 24, 123-135.

Jacek Mlochowski, Halina Wojtowicz, 2015. Developments in Synthetic Application of Selenium(IV) Oxide and Organoselenium Compounds as Oxygen Donors and Oxygen-Transfer Agents. Molecules 20, 10205-10243

Kaczara P, Sarna Tadeusz, Burke J, 2010. Dynamics of H_2O_2 availibility to ARPE-19 cultures in models of oxidative stress . Free Radical Biology & Medicine. 48, 1064–1070.

Käsdorf B.T., Arends F., Lieleg O., 2015. Diffusion Regulation in the Vitreous Humor. Biophys. J. 109, 2171–2181.

Kodama T, Tomita, N, Horie S, Sax N, Iwasaki H, Suzuki R, Maruyama K, Mori S, Manabu F, 2010. Morphological study of acoustic liposomes using transmission electron microscopy. J. Electron Microsc. (Tokyo). 59, 187–196.

Lin T.C., Hung K.H., Peng C.H., Liu J.H., Woung L.C., Tsai C.Y., Chen S.J., Chen Y.T., Hsu C., 2015. Nanotechnology-based drug delivery treatments and specific targeting therapy for age-related macular degeneration. J. Chinese Med. Assoc. 78, 635–641.

Mandai M, Watanabe A, Kurimoto Y, Hirami Y, Morinaga C, Daimon T, Fujihara M, Akimaru H, Sakai N, Shibata Y, Terada M, Nomiya Y, Tanishima S, Nakamura M, Kamao H, Sugita S, Onishi A, Ito T, Fujita K, Kawamata S, Go M.J, Shinohara C, Hata K, Sawada M, Yamamoto M, Ohta S, Ohara Y, Yoshida K, Kuwahara J, Kitano Y, Amano N, Umekage M, Kitaoka F, Tanaka A, Yoshida K, Kuwahara J, Kitano Y, Amano N, Umekage M, Kitaoka F, Tanaka A, Okada C, Takasu N, Ogawa S, Yamanaka S, Takahashi M, 2017.Autologous Induced Stem-Cell-Derived Retinal Cells for Macular Degenration . The New England Journal of Medicine 11, 376-385.

Parvini M, Satarian L, Parivar K, Javan M, Tondar M, Ahmad S, Baharvand H, 2014. Human pluripotent stem cell-derived retinal pigmented epithelium in retinal treatment: from bench to bedside. Mol Neurobiol 50, 597-612.

Peter C. Raich, Junxuan Lu, Henry J. Thompson, 2001. Selenium in cancer prevention: clinical issues and implications. Cancer Investigation. 19, 540–553.

Rafique J., Saba S., Canto R.F.S., Frizon T.E.A., Hassan W., Waczuk E.P., Jan M., Back D.F., Rocha J.B.T. Da, Braga A.L., 2015. Synthesis and biological evaluation of 2-picolylamide-based diselenides with non-bonded interactions. Molecules 20, 10095–10109.

Rania Hathout, Samar Mansour, 2007 Liposomes as an Ocular Delivery System for Acetazolamide: In Vitro and In Vivo Studies.AAPA PharmSciTech 8,1.

Roth F., Bindewald A., Holz F.G., 2004. Keypathophysiologic pathways in age-related macular disease. Graefe's Arch. Clin. Exp. Ophthalmol. 242, 710–716.

Sahoo S.K., Dilnawaz F., Krishnakumar S., 2008. Nanotechnology in ocular drug delivery. Drug Discov. Today 13, 144–51.

Sharman W.M., Allen C.M., Lier J.E. Van, 1999. Photodynamic therapeutics : basic principles and clinical applications. Drug Discovery Today. 4, 507–517.

Shen Y., Tu J., 2007. Preparation and ocular pharmacokinetics of ganciclovir liposomes. AAPS J. 9, E371–E377.

Schewe T, 1994. Molecular actions of Ebselen—an antiinflammatory antioxidant, General Pharmacology: The Vascular System 26, 1153-1169.

Song C.C, Du F.S., 2014. Oxidation-responsive polymers for biomedical applications. J. Mater. Chem. B. 2, 3413-3426.

Schwartz SD, CD Regillo, BL Lam, D Eliott, PJ Rosenfeld, NZ Gregregori, JP Hubschman, JL Davis, G Heilwell, M Spirn, J Maguire, R Gay, J Bateman, RM Ostrick, D Morris, M Vincent, E Anglade, LV Del Priore and R Lnaza, 2015.Human embryonic stem cell-derived retinal pigment epithelium in patients with age-related macular degeneration and Stargardt's macular dystrophy: follow-up of two open-label phase ½ studies. Lancet 16, 385-509.

Tate D.J., Miceli M. V, Newsome, D. a, 1995. Phagocytosis and H2O2 induce catalase and metallothionein gene expression in human retinal pigment epithelial cells. Invest. Ophthalmol. Vis. Sci. 36, 1271–1279.

Thrimawithana Thilini, Young Simon, Bunt Craig, Green C, Alany R, 2011. Drug delivery to the posterior segment of the eye.. Drug Discovery Today. 16, 270-277.

Torchilin V.P., 2014. Multifunctional, stimuli-sensitive nanoparticulate systems for drug delivery. Nat. Rev. Drug Discov. 13, 813–827.

Zahabi A., Shahbazi E., Ahmadieh H., Hassani S.-N., Totonchi M., Taei A., Masoudi N., Ebrahimi M., Aghdami N., Seifinejad A., Mehrnejad F., Daftarian N., Salekdeh G.H., Baharvand H., 2012. A New Efficient Protocol for Directed Differentiation of Retinal Pigmented Epithelial Cells from Normal and Retinal Disease Induced Pluripotent Stem Cells. Stem Cells Dev. 21, 2262–2272.

Zalipsky S., Qazen M., Walker J.A., Mullah N., Quinn Y.P., Huang S.K., 1999. New detachable poly(ethylene glycol) conjugates: Cysteine-cleavable lipopolymers regenerating natural phospholipid, diacyl phosphatidylethanolamine. Bioconjug. Chem. 10, 703–707.

Figure legends

Figure 1. The schematic illustration of liposomal drug delivery effect on hESC-RPE and mechanism of drug release from responsive liposome in redox environment.

Figure 2. Synthesis scheme of diselenide (A) ^{1}H-NMR spectra of 10-bromodecanoic acid (I) and diselenide (II)(B), and FTIR of diselenide (C).

Figure 3. Evaluation of the optimal formulation for liposomes. We measured the intensity of released carboxyl fluorescence at 488 nm excitation and emission from the CF loaded liposomes when exposed to different concentrations of H_2O_2 (0-800 µM). Two groups of liposomes (DMPC and Egg PC/DOPE) with different concentrations of SeSe were studied. DMPC release, DMPC/10% SeSe, DMPC/20% SeSe , Egg PC/DOPE, Egg PC/DOPE/10% SeSe, and Egg PC/DOPE/20% SeSe (A). Transmission electron microscopy (TEM) images of negatively stained liposomes (Egg PC/DOPE) at 8000x magnification on the left (I) and 31500x magnification on the right (II) (B). Egg PC: Egg/L-α-phosphatidylcholine; DOPE: 1,2-dio-leoyl-sn-glycero-3-phosphoethanolamine; DMPC: 1,2-dimyristoyl-sn-glycero-3-phosphocholine; SeSe: Diselenide.

Figure 4. Release of N-acetyl cysteine (NAC) from Lip2 (Egg PC/DOPE/20% SeSe), Lip1 (Egg PC/DOPE/10% SeSe), and Egg PC/DOPE when exposed to 0.1 wt. % H_2O_2 buffer. HPLC assay was used to measure NAC release. Release from carriers that contained liposomes were significantly higher than carriers without SeSe. Data presented as mean±SD. *: $P<0.05$; **:

P<0.01 Egg PC: Egg/L-α-phosphatidylcholine; DOPE: 1,2-dio-leoyl-sn-glycero-phosphoethanolamine; SeSe: Diselenide.

Figure 5. hESC-RPE cells characterization and cell metabolic activity assay**.** hESC-RPE cells characterization and cell metabolic activity assay. Phase- contrast image of hESC- derived RPE, 10 days after passage 1(A) hESC-RPE recover its hexagonal morphology (B) the fluorescent image showing phagocytosis of green fluorescent beads by hESC- derived pigmented cells (C). Representative immunostaining images of hESC-RPE cells at passage 1 analyzed for typical mature RPE protein; RPE65 (D). Cell metabolic activity of RPE cells when treated with different concentrations of H_2O_2. Nuclei were counterstained with DAPI (D). Scale bar: 50 µm (A- C) and 100 µm (D-F). Effects of drug and carriers on hESC-RPE cells. MTS assay of Lip1, Lip2, and Egg PC/DOPE [with or without N-acetyl cysteine (NAC)] on passage-1 hESC-RPE cells after 24 h. No significant toxicity of the carriers was observed (G). Cell metabolic activity of hESC-RPE cells for oxidative stress modeling after exposure to different concentrations of H_2O_2 (0-750 µM). Significant difference was observed for the 200 µM and 500 µM groups (H). Student's *t*-test. *: P<0.05; **: P<0.01.

Figure 6. MTS assay of hESC-RPE cells. The cells were treated with different concentrations of H_2O_2 (0 µM, 200 µM, and 500 µM) exposed to N-acetyl cysteine (NAC; 10 mM), Lip2/NAC (Egg PC/DOPE/20% SeSe), and Lip1/NAC (Egg PC/DOPE/10% SeSe). Total concentration of NAC was 10 mM. Values are the mean±standard deviation (SD). *: P<0.05; **: P<0.01; ***: P<0.001. Data are written as the mean±SD. Egg PC: Egg/L-α-phosphatidylcholine; DOPE: 1,2-dio-leoyl-sn-glycero-3-phosphoethanolamine; SeSe: Diselenide.

Figure 7. Expression of several oxidative stress-related genes (*SOD1*, *SOD2*, and *CAT*) and control, GAPDH. The gene expressions were measured in hESC-RPE cell oxidative stress modeled using 0.1 wt. % H_2O_2. The cells were treated with NAC (10 mM), Lip2/NAC (Egg PC/DOPE/SeSe 20%), Lip1/ NAC (Egg PC/DOPE/SeSe 10%), or left untreated. Control group were not treated with 0.1 wt. % H_2O_2. *SOD1* activity has reached normal level when treated with smart liposomes. *SOD2* activity has reached normal level when treated with smart liposomes. *CAT* activity has reached normal level when treated with smart liposomes. Data (means of triplicates) standard deviations are represented. Data normalized with GAPDH as house keeping gene. *$p<0.05$, ** $p<0.01$, *** $p < 0.001$. Data represent the mean ± SD.

Table legends

Table 1. Physical properties and entrapment efficiency of liposomes (n=3).

Formulation	Average size (nm)	Zeta potential (mV)	PDI*	Entrapment efficiency (EE, %)
Egg PC/DOPE	156.0±3.3	-3.51±0.5	0.099±0.006	-
Lip1	144.8±2.75	-20.5±2.25	0.083±0.0057	-
Lip2	145.8±5.7	-22.7±1.7	0.155±0.021	-
Egg PC/DOPE-NAC	176.3±4.43	-3.53±0.6	0.178±0.01	12.3
Lip1-NAC	182.1±3.7	-17.8±2.3	0.141±0.002	11.8
Lip2-NAC	223.3±2.89	-20.9±2.3	0.222±0.001	11.45

*PDI: Polydispersity index. Egg PC: Egg/L-α-phosphatidylcholine; DOPE: 1,2-dio-leoyl-sn-glycero-3-phosphoethanolamine; NAC: N-acetyl cysteine

Table. S1. List of primers for real-time PCR used in this study.

Gene	Accession Number	Primer forward 5′-3′	Primer reverse 5′-3′
SOD1	NM:000454	AGGGCATCATCAATTTCGAGC	GCCCACCGTGTTTTCTGGA
SOD2	NM:000636	AACCTCAGCCCTAACGGTG	AGCAGCAATTTGTAAGTGTCCC
CAT	NM:001752	ACTTTGAGGTCACACATGACATT	CTGAACCCGATTCTCCAGCA
GAPDH	NM:002046	CTCATTTCCTGGTATGACAACGA	CTTCCTCTTGTGCTCTTGCT

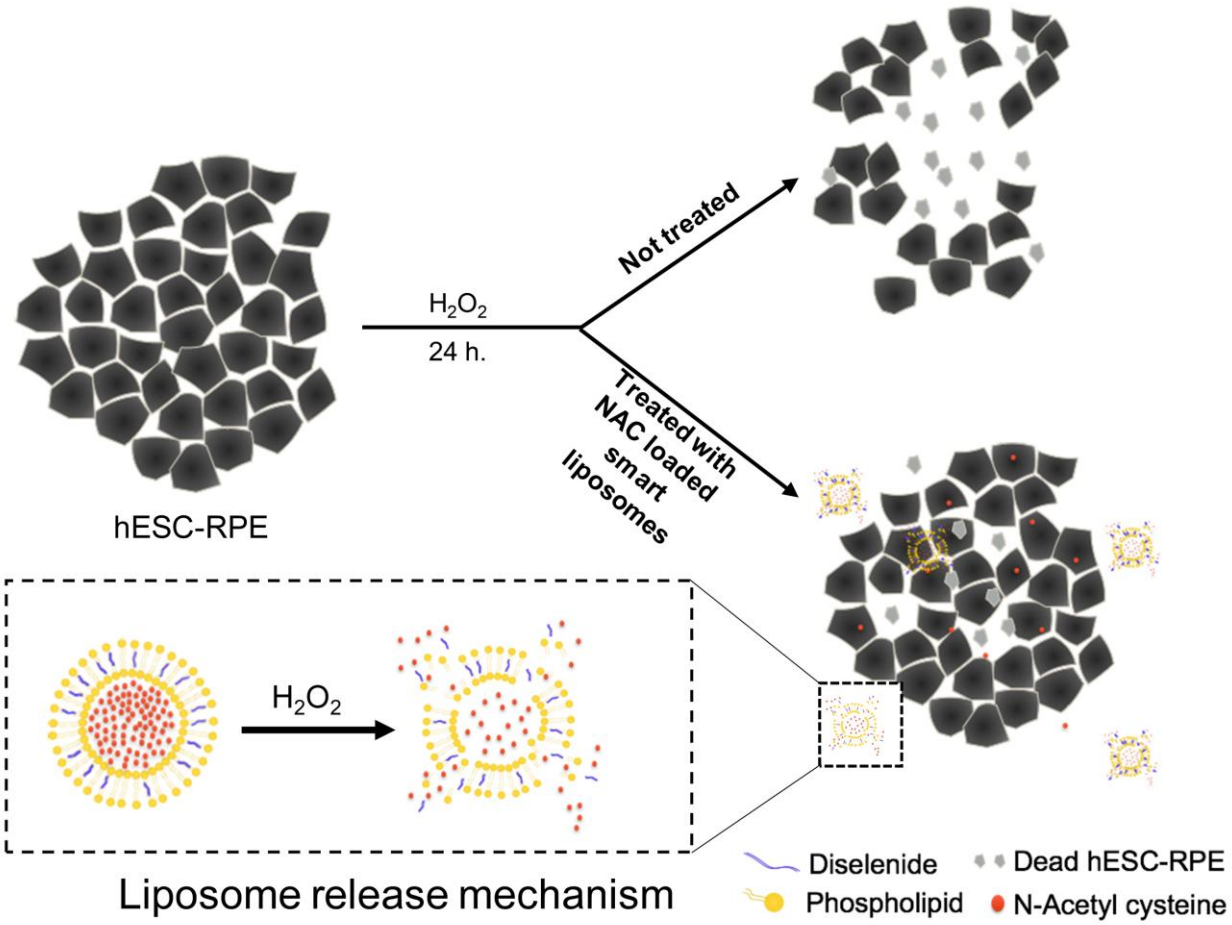
H_2O_2
24 h.
Not treated
Treated with NAC loaded smart liposomes
hESC-RPE
H_2O_2
Liposome release mechanism
Diselenide
Phospholipid
Dead hESC-RPE
N-Acetyl cysteine

A

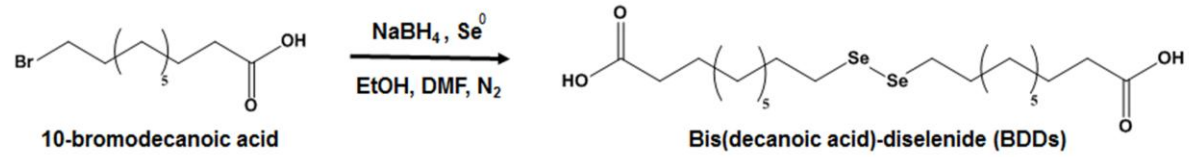

10-bromodecanoic acid

Bis(decanoic acid)-diselenide (BDDs)

B

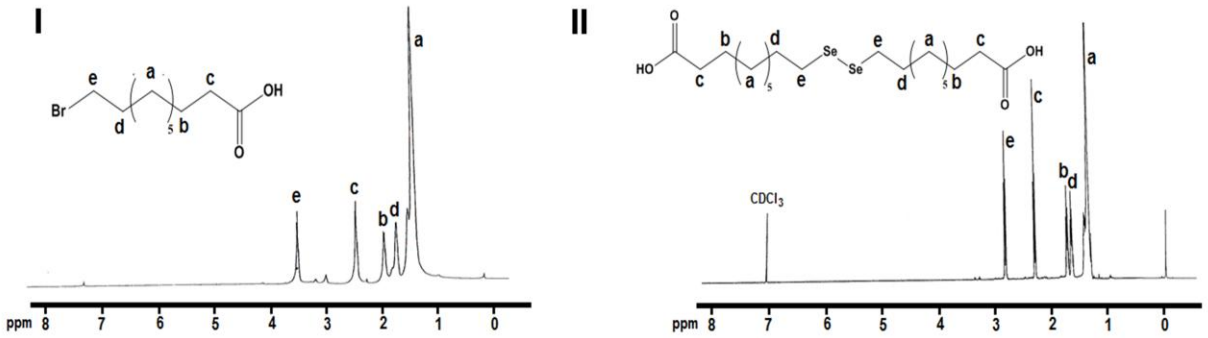

C

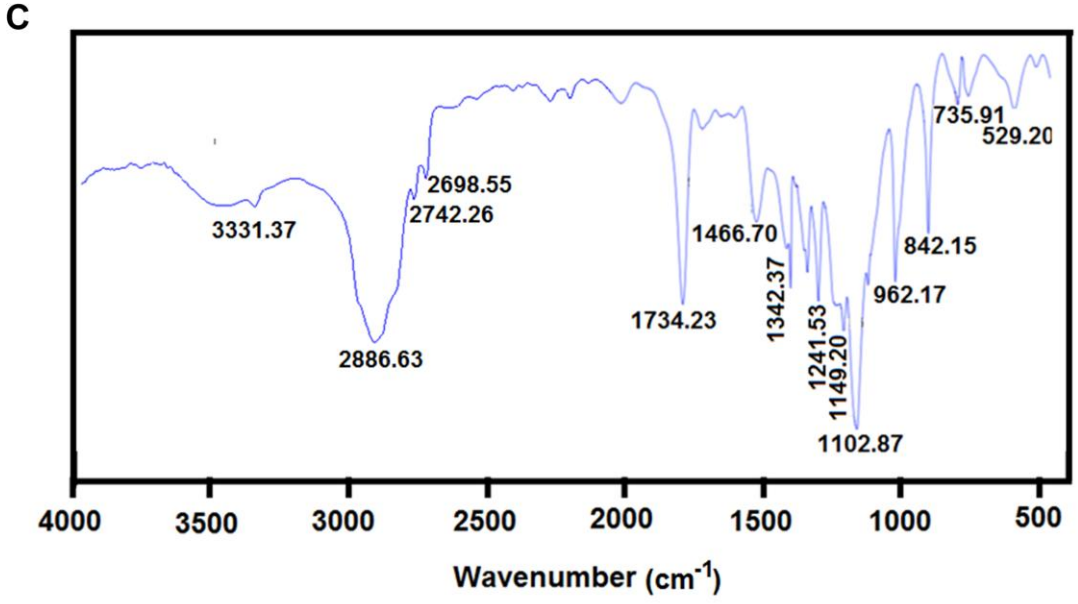

A

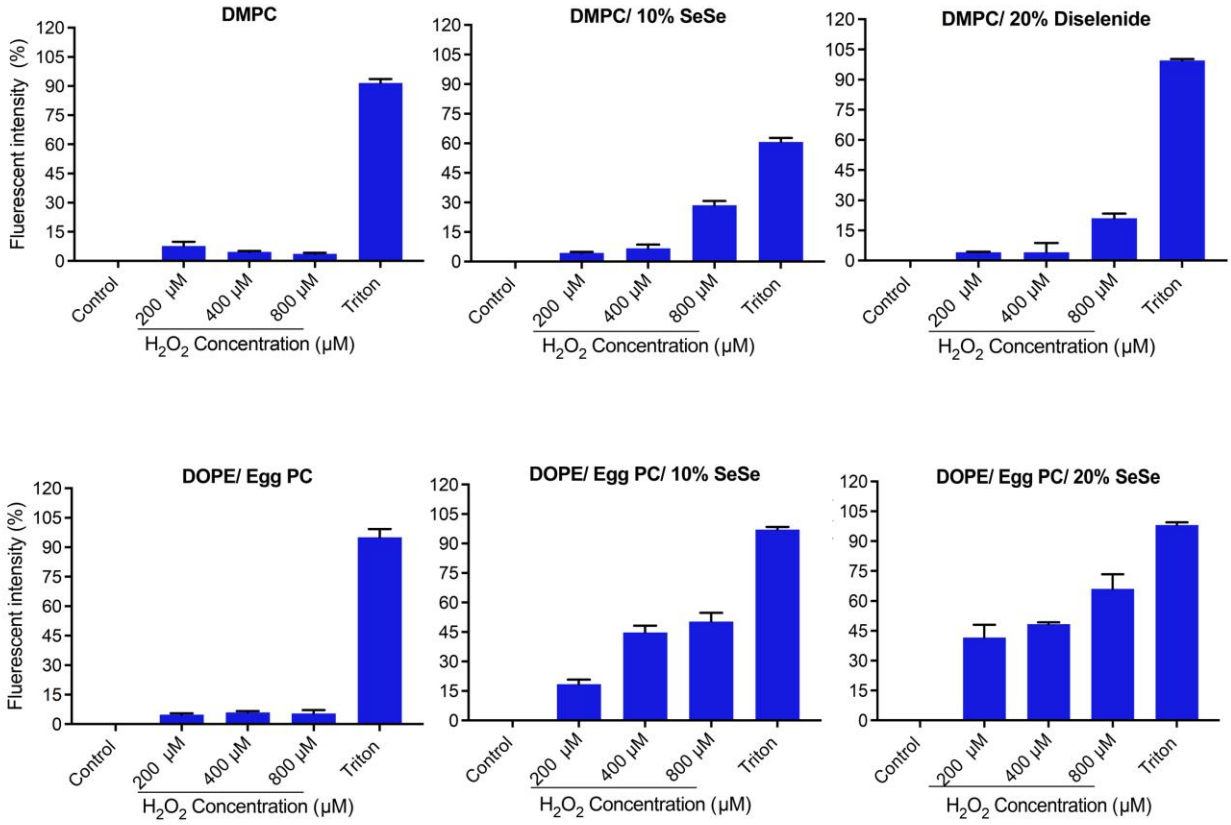
DMPC
DMPC/ 10% SeSe
DMPC/ 20% Diselenide
DOPE/ Egg PC
DOPE/ Egg PC/ 10% SeSe
DOPE/ Egg PC/ 20% SeSe
Fluorescent intensity (%)
0
15
30
45
60
75
90
105
120
Control
200 µM
400 µM
800 µM
Triton
H2O2 Concentration (µM)

B

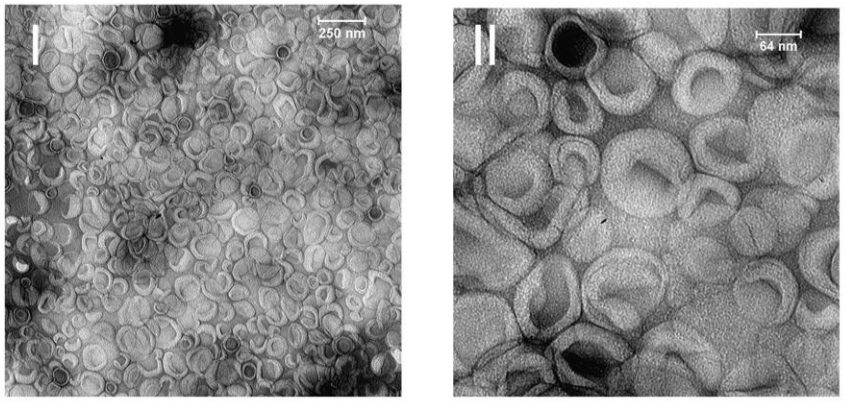
I
250 nm
II
64 nm

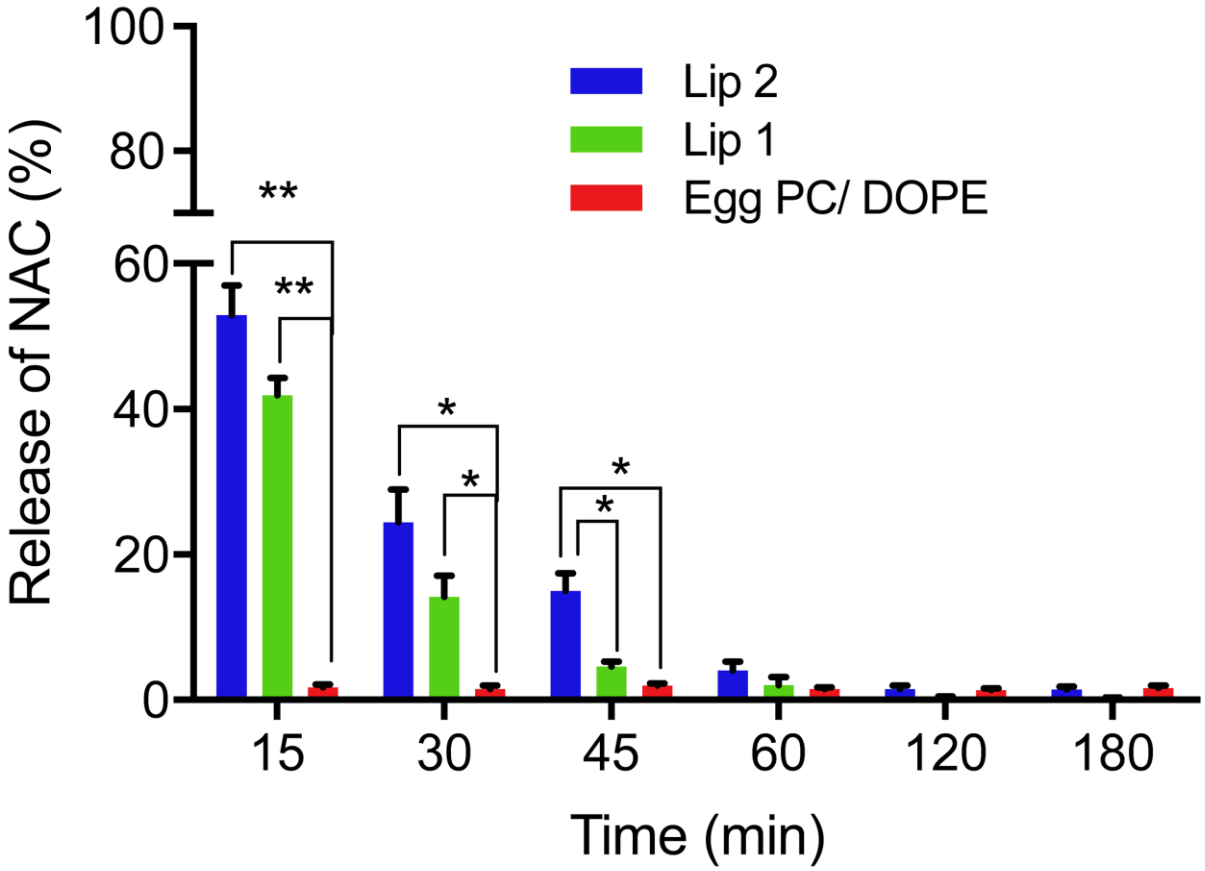
100
80
60
40
20
0
Release of NAC (%)
Lip 2
Lip 1
Egg PC/ DOPE
**
**
*
*
*
*
15
30
45
60
120
180
Time (min)

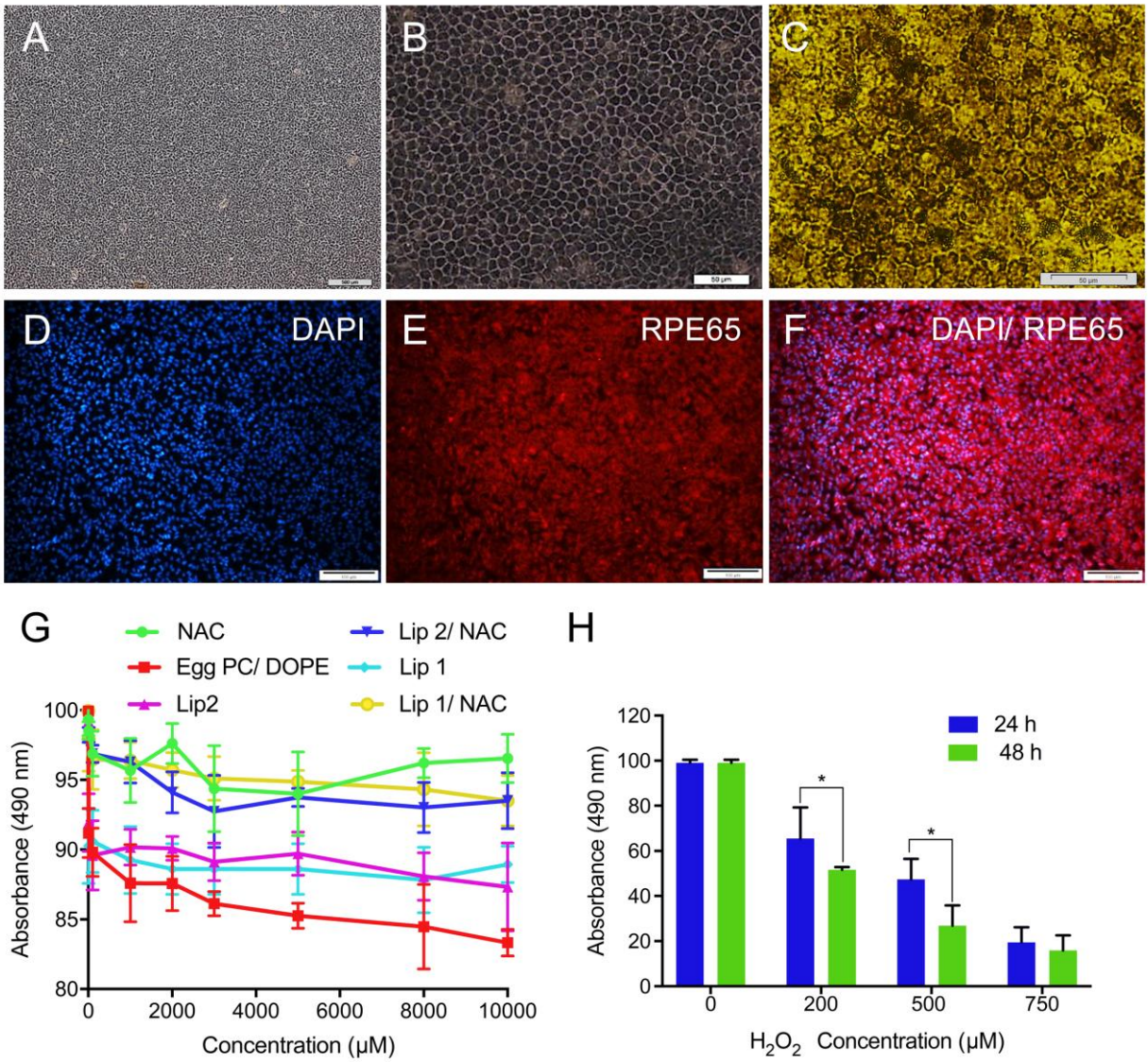
A
B
C
D
DAPI
E
RPE65
F
DAPI/ RPE65
G
NAC
Egg PC/ DOPE
Lip2
Lip 2/ NAC
Lip 1
Lip 1/ NAC
Absorbance (490 nm)
Concentration (μM)
H
24 h
48 h
Absorbance (490 nm)
H2O2 Concentration (μM)

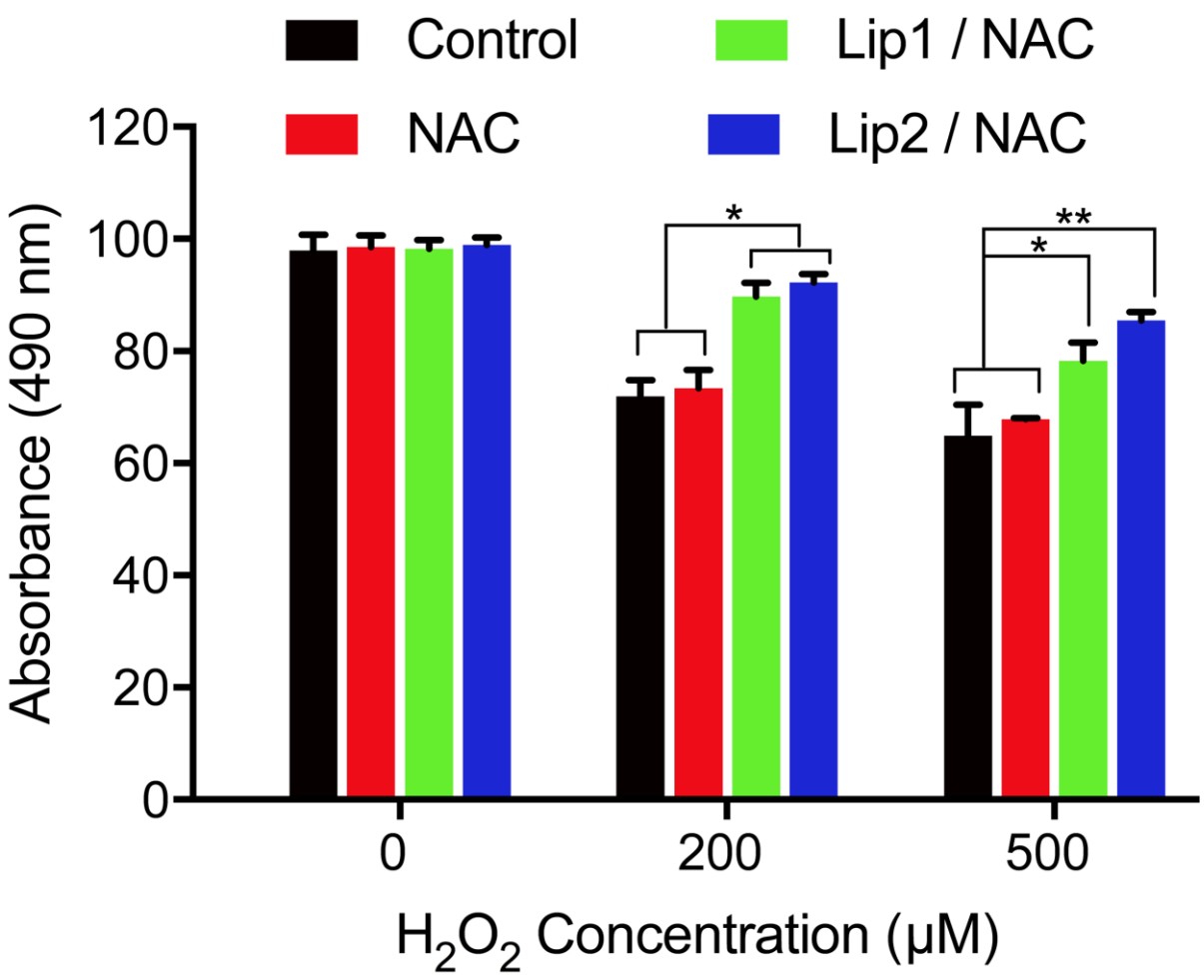
Control
Lip1 / NAC
NAC
Lip2 / NAC
120
100
80
60
40
20
0
Absorbance (490 nm)
*
**
*
0
200
500
H2O2 Concentration (μM)

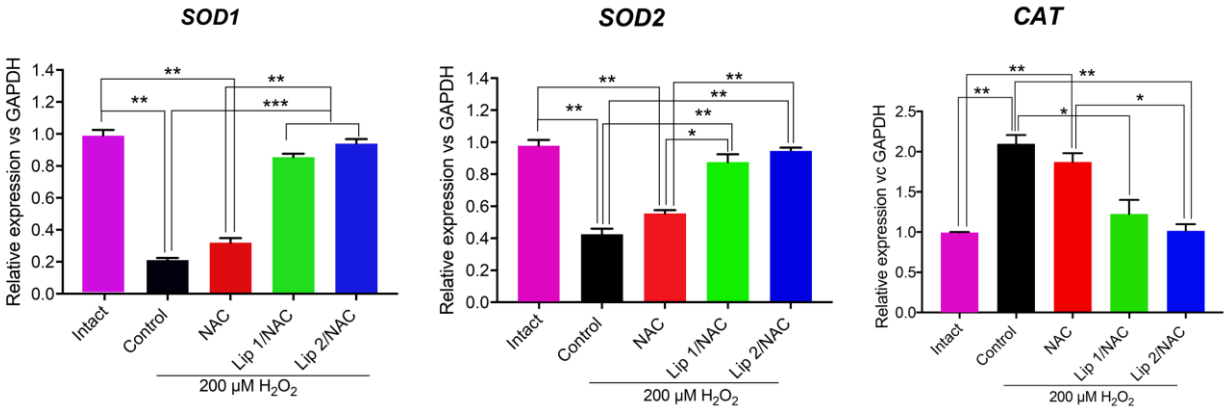

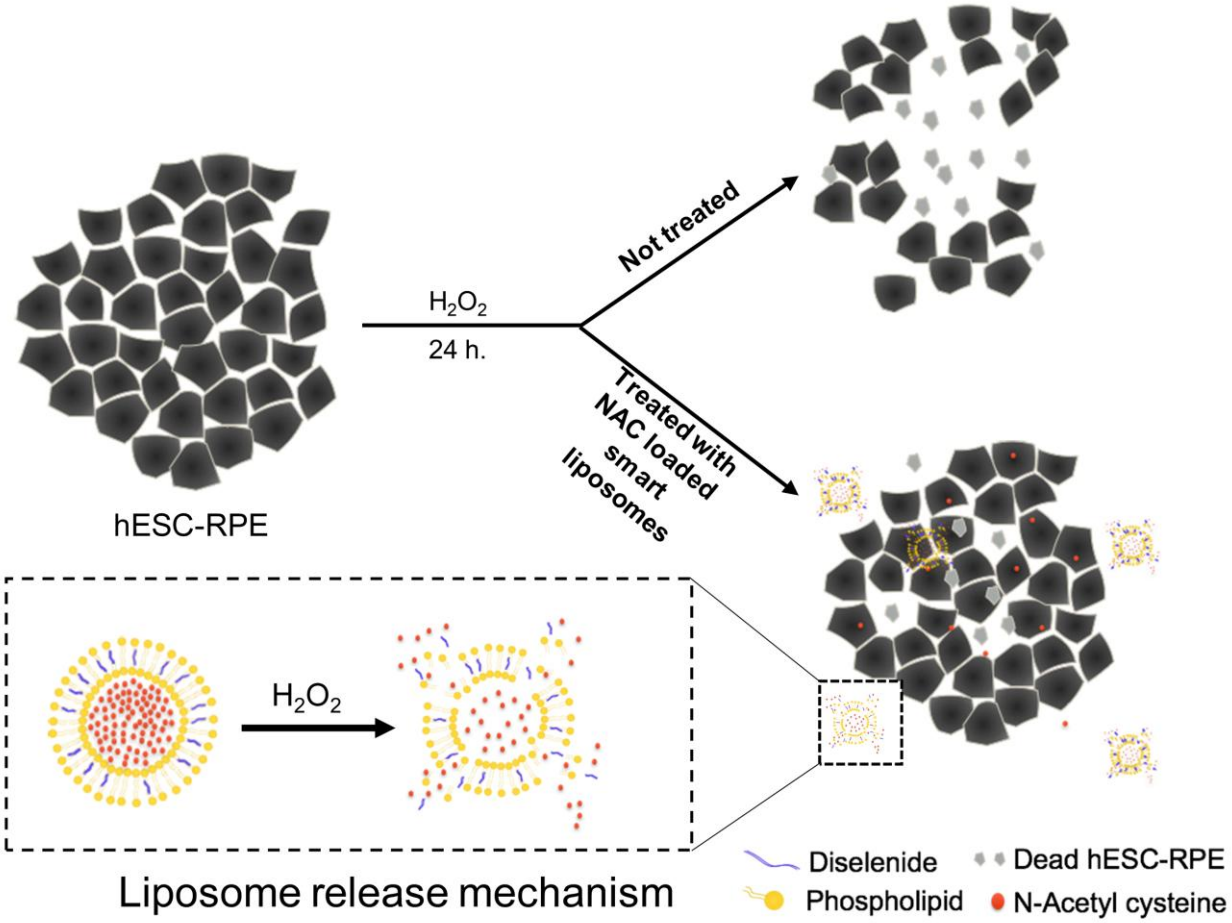
H_2O_2
24 h.
Not treated
Treated with NAC loaded smart liposomes
hESC-RPE
H_2O_2
Liposome release mechanism
Diselenide
Phospholipid
Dead hESC-RPE
N-Acetyl cysteine